Eur. Phys. J. B **47**, 177–184 (2005)
DOI: 10.1140/epjb/e2005-00329-6

THE EUROPEAN PHYSICAL JOURNAL B

Quantum microscopic vs. classical macroscopic calculations on the phenomenon of electrostatic influence

B. Blaive[a], A. Julg[†], and A. Pellegatti

CNRS, Case A62, Université Paul Cézanne, Faculté de Saint-Jérôme, 13397 Marseille Cedex 20, France

Received 13 May 2005
Published online 11 October 2005 –

Abstract. In order to compare microscopic and macroscopic approaches to the phenomenon of electrostatic influence, we have studied the atomic charges of an electric conductor, obtained either from macroscopic classical electrostatics, or microscopic quantum ab initio calculations. A torus was chosen as conducting material, built from valence monoelectronic atoms and influenced by an external point charge. The classical electric charges are obtained by integrating the macroscopic density over "atomic" sectors. This density is determined from a numerical integration of linearized electrostatic equations. The quantum charges are defined from Natural Orbitals in MP2/6-31G* calculations on clusters of different sizes. The overall agreement is good, with reasonable discrepancies due (i) to the continuity of the macroscopic model, which ignores the oscillations on atomic distances; and (ii) to the linearity constraint in the macroscopic equations.

PACS. 31.15.Ar Ab initio calculations – 41.20.Cv Electrostatics; Poisson and Laplace equations, boundary-value problems – 71. Electronic structure of bulk materials

1 Introduction

In the presence of fixed external electric charges, a conducting body is subjected to electrostatic influence: a surface charge density appears on the surface of the conductor, so that the total electric field remains equal to zero inside the conductor. This phenomenon is usually discussed in terms of macroscopic bodies, and described by macroscopic electrostatic equations [1–3]. In this paper, we address the question of the relevance of quantum microscopic calculations for describing electrostatic influence. For this purpose, we will use ab initio quantum calculations on sufficiently large numbers (6 to 90) of small atoms, i.e. hydrogen or sodium, clusters. The atomic charges obtained with quantum mechanics will be compared [4] to the macroscopic charge density deduced from the classical macroscopic electrostatic equations (linear terms).

(1) *Shape of the conductor.* The conductor geometry must be chosen with a small volume in relation to its surface area, so that the number of atoms necessary to fill the conductor will be small enough for precise quantum calculations. Linear volumes (a rod, a torus) satisfy this condition. We have chosen a torus rather than a rod, the extremities of which would generate strong electrostatic field variations. Microscopically, a torus can be realized with a single ring of atoms, with its 3D-delocalized electronic cloud. Apart from its overall size, the shape of a torus depends on a unique parameter, i.e. the ratio $\rho = r/R$ of the section radius r to the mean radius R ($\rho < 1$). In the following, r and R should vary according to the kind of atom chosen, and to their number N. In the macroscopic calculations, the section radius r is chosen equal to half the interatomic distance d between neighbouring atoms, except otherwise stated (cf. Sect. 4.2).

(2) *Conductor material.* Because a large number of quantum ab initio calculations are to be performed, atoms with a small number Z of electrons must be chosen. We will treat several rings (N = 6, 18, 30, 50, 90) of hydrogen atoms ($Z = 1$), and one ring ($N = 18$) of sodium atoms ($Z = 11$). The quantum orbitals which will be found justify their being considered as conducting materials. Therefore, in the macroscopic calculations, the continuity equation

$$\varepsilon_0 \mathbf{E}_n(\text{ext}) = \varepsilon \mathbf{E}_n(\text{int}) \qquad (1)$$

($\mathbf{E}_n$ is the normal electric field, taken on the two sides of the torus surface and ε_0 is the vacuum dielectric constant) must be written with an infinite dielectric constant ε, i.e. $\mathbf{E}_n(\text{int}) = 0$.

(3) *External charge.* The torus is influenced by a unique external electric point charge Q, placed in the plane of the torus. This position can be described either

[a] e-mail: bruno.blaive@univ.u-3mrs.fr

[†] Deceased on March 14th 2003

by the absolute distance D from Q to the torus center, or by the relative distance R/D.

The value of the charge Q is unimportant for classical macroscopic calculations, the linear results of which are proportionnal to Q. Therefore, classical calculations will be performed for only one value, $Q = -1$ (e^-: electron charge atomic unit). The value of Q will be varied in the quantum calculations, the results of which are not linear in Q.

2 Classical macroscopic calculation

The calculation consists of two parts. We have first to find the surface charge density σ on the torus, using the fact that inside the torus it creates a field $-E_Q$ opposite to that created by Q, and then to integrate the charge density σ over each of N equal toroidal sectors representing the atoms.

(1) *Approximation of* σ. In principle an analytical calculation of σ is possible, using toroidal functions [5,6]. But handling these functions is heavy, and their numerical surface integration over the toroidal sectors would be rather time-consuming. Therefore, we choose to approximate σ by a limited Fourier expansion,

$$\sigma^{\text{approx}}(\theta,\varphi) = \sum_{m,n} a_{mn}\cos(\mathrm{m}\theta)\cos(\mathrm{n}\varphi), \tag{2}$$

where $0 \le \theta < 2\pi$ and $0 \le \varphi < 2\pi$ are toroidal coordinates (θ on the section circle of radius r, φ on the circle of radius R). For symmetry reasons the coefficients of the sinus terms are zero. For computing the field created at any point $\mathbf{S}$ inside the torus, the surface charge distribution (2) is replaced by a regular distribution of point charges $\mathbf{q}$ on the torus surface. A grid of 128×256 point charges $\mathbf{q}_{ij}$ is chosen at the summits of a toroidal net with the following toroidal coordinates:

$$\mathbf{q}_{ij} : (r; \theta_i = i2\pi/128; \varphi_j = j2\pi/256).$$

(2) *Electrostatic condition.* The coefficients a_{mn} in expansion (2) are optimized in order to minimize the modulus of the total electric field

$$\mathbf{E} = \mathbf{E}_Q + \mathbf{E}_\sigma \tag{3}$$

inside the conductor. More precisely, we minimize the squared modulus of $\mathbf{E}$, summed over a number of fixed points $\mathbf{S}$ chosen inside the conductor, i.e.

$$\Delta = \sum_{\mathbf{S}} \mathrm{E}^2(\mathbf{S}). \tag{4}$$

In definition (4) the summation is extended over a second toroidal net

$$\mathbf{S}_{ij} : (r \times 0.8; \theta_i = (i+1/2)\pi/32; \varphi_j = (j+1/2)\pi/64),$$

inside the torus. The 1/2 coefficient introduces an infinitesimal shift which ensures that the positions of the two nets are symmetrical with respect to each other.

(3) *Linear optimization.* Δ is a second order polynomial of the coefficients a_{mn}. Therefore, a linear optimization is possible. To avoid double indexing in summation (4), let us denote a pair of indices (m,n) occuring in (2) by a single index M and similarly M' for a pair (m',n'). The equations

$$\partial\Delta/\partial a_M = 0$$

lead to the system of linear equations

$$a_M C_{MM} + \sum_{M' \ne M} a_{M'} C_{MM'} + K_M = 0, \tag{5}$$

with

$$C_{MM'} = \sum_{\mathbf{S}} \mathbf{V}_M(\mathbf{S}) \cdot \mathbf{V}_{M'}(\mathbf{S}) \tag{6}$$

$$K_M = \sum_{\mathbf{S}} \mathbf{V}_M(\mathbf{S}) \cdot \mathbf{B}(\mathbf{S}) \tag{7}$$

and

$$\mathbf{V}_M(\mathbf{S}) = \sum_{\mathbf{q}} [R + r\cos\theta_{\mathbf{q}}]\cos(m\theta_{\mathbf{q}})\cos(n\varphi_{\mathbf{q}})(\mathbf{S}-\mathbf{q})|\mathbf{S}-\mathbf{q}|^{-3} \tag{8}$$

$$\mathbf{B}(\mathbf{S}) = Q(r\Delta\theta\Delta\varphi)^{-1}(\mathbf{S}-\mathbf{Q})|\mathbf{S}-\mathbf{Q}|^{-3}. \tag{9}$$

The coefficients (6) and (7), which necessitate two (twofold) summations $\sum_{\mathbf{S}}$ and $\sum_{\mathbf{q}}$ over the internal and surface toroidal nets, are computed once and for all. The computer program *ElstTore* was written for this purpose. With a Fourier expansion (2) limited to order six, i.e. to twenty seven coefficients a_{mn}, the precision is satisfactory: at the end of the optimization, the residual value of Δ is one or two per cent of the sum

$$\Delta_{\text{initial}} = \sum_S E_Q^2(\mathbf{S}) \tag{10}$$

which is the starting value of Δ when all the a_{mn}'s are initialized to zero.

Note that the first and second coefficients a_{00} and a_{10} are connected together. Indeed the total charge of the torus is

$$q_{\text{torus}} = 2\pi^2 r(2R\,a_{00} + r\,a_{10}), \tag{11}$$

which gives for an uncharged torus

$$a_{00} = -r/(2R)a_{10}. \tag{12}$$

(4) *Integration of* σ *over equal toroidal sectors,* representing the atoms. The n-th toroidal sector can be defined by

$$\varphi_{\min}(n) < \varphi < \varphi_{\max}(n), \quad \text{any} \quad 0 \le \theta < 2\pi. \tag{13}$$

with

$$\varphi_{\min}(n) = (n-3/2)2\pi/n; \varphi_{\max}(n) = (n-1/2)2\pi/n.$$

When integrating relation (2) over this region, we find that the global charge of the sector is

$$q_n = \pi r[(2Ra_{00} + ra_{10})(\varphi_{\max} - \varphi_{\min}) + \sum_{p>0}(2Ra_{0p} + ra_{1p})[\sin(p\varphi_{\max}) - \sin(p\varphi_{\min})]/p, \quad (14)$$

the first term of which is zero thanks to relation (12).

3 Quantum microscopic approach

In quantum chemical calculations the best suited level of theory to obtain reliable electronic charge [7] is the Moller-Plesset perturbation method at order 2 combined with basis sets of double-ζ plus polarization quality as the 6-31G* basis set [8]. For computing reasons, we would rather deal with the lightest atoms possible, provided that the physical conditions of the solid phases are fulfilled. Therefore we have chosen sodium, whose solid phase has a metallic character at ambient temperature, and hydrogen, although its metallic character appears only in a solid phase under extreme conditions of pressure and temperature. It is important that we obtain molecular orbitals (MO) having a metallic character. This is achieved first by the choice of a torus, which fulfils the infinite boundary conditions, and moreover by the consideration of equal distances between bonded atoms. Indeed, if we optimize the geometry while starting from a distorted Peierls-like structure, where H_2 molecule interatomic distances are preserved, we can show that, without obtaining any energy minimum point on the potential energy surface, we tend to infinitely separated H_2 molecules.

To measure the consequences of the use of a limited number of atoms, we need to test the convergence of the results according to the number of atoms N. We select values of N (N = 6, 18, 30, 50 and 90) giving electronic closed-shells. With valence monoelectronic atoms this leads to the condition that $(N-2)$ must be a multiple of 4, since all MO's are doubly degenerate except the first one. For the isolated torus without an external charge ($Q = 0$), and for each value of N, the optimization of the structure at the MP2/6-31G* level yields an almost linear variation of the radius of the torus in function of the number of atoms (Tab. 1), since the distance (d) between bonded hydrogens, and the MP2 atomization energy per atom ($E_{\rm at}/N$), are nearly constant. Although a six atom ring is far from representing an infinite solid, the $N = 6$ case does not differ much from the others, when we examine the distances and the energy (Tab. 1). In the benzene molecule, a completely different case, the well-known aromatic properties of the π system also result *in fine* in C-C distances all equal, and suggest that the"metallic character" can be already present in as few as six atoms.

The geometry optimized in the quantum approach is used also in the macroscopic calculations.

In presence of an external point charge, we keep the same interatomic distances in the torus. The point charge Q is taken aligned with one atom (numbered 1), i.e. on a diameter containing the centre of one atom.

Table 1. Optimized torus radius R (Å), interatomic H-H distances d (Å) and atomization energies $E_{\rm at}$ per atom (kcal/atom) of N-atoms circular clusters of hydrogens obtained at the MP2/6-31G* level.

N	6	18	30	50	90
R	0.9757	2.7830	4.6317	7.7176	13.8911
R/N	0.1626	0.1546	0.1544	0.1544	0.1544
d	0.9757	0.9665	0.9683	0.9692	0.9696
$E_{\rm at}/N$	38.02	36.87	36.51	39.39	36.36

As is well known, atomic partial charges are not uniquely defined. Here we will consider the charges derived from a Natural Population Analysis (NPA) [9] where the natural-orbital occupation numbers are obtained from the diagonalization of the one-electron density matrix. GAUSSIAN 98 software has been used throughout this work [10].

4 Results

4.1 Hydrogen atom conductor

(i) The microscopic and macroscopic charges are tabulated or figured in the following cases: $N = 6, R/D = 0.55$ to 0.1 (Tab. 2); $N = 18, R/D = 0.55$ and 0.4 (Figs. 1 and 2); $N = 30$, $R/D = 0.55$ and 0.4 (Figs. 3 and 4); $N = 50, R/D = 0.55$ (Fig. 5); and $N = 90, R/D = 0.55$ (Fig. 6).

The most striking feature of the microscopic and macroscopic curves representing the atomic charges along the torus, is that they are similar in all cases. They almost coïncide when Q is not too close to the torus, i.e. for $R/D = 0.4$ or smaller. When Q is close, the general shapes of the curves are identical, but periodic discrepancies occur, due to microscopic or macroscopic oscillations that will be discussed later.

For a negative external charge $Q = -1$, the charge on the torus has a maximum on atom 1, in the closest position to Q, and it decreases along the torus, down to a minimum on the diametrally opposite position (atom $N/2+1$). Therefore, in function of the angular coordinate φ of the torus ($0 < \varphi < 2\pi$), the surface charge has the shape of a well, which is rather square when Q is close ($R/D = 0.55$) and thinner when Q is far ($R/D = 0.4$). As explained in Section 2, the macroscopic charges on the torus are proportional to Q, but the microscopic ones are not (Tab. 2).

Microscopic oscillations are observed on several curves, especially for small N, with a periodic length corresponding to two atoms (alternation). Their amplitude is greater when Q is close : 5×10^{-2} (e^-) for $n = 18$, $R/D = 0.7$ (not represented here); 10^{-2} for $N = 18$, $R/D = 0.55$ (Fig. 1), invisible for $R/D = 0.4$ (Fig. 2); for $N = 30$ the amplitude is 2×10^{-2} for $R/D = 0.55$ (Fig. 3), invisible for $R/D = 0.4$; for $N = 50$ it is 2×10^{-3} for

Table 2. Natural orbital charges (10^{-4} e$^-$) of hydrogen atoms on a six-membered ring (radius R) under the influence of a fixed negative point charge Q (e$^-$) lying at a distance D from the center of the circle. Values in brackets are those obtained from the macroscopic treatment.

Q	R/D	Q_1	$Q_2 = Q_6$	$Q_3 = Q_5$	Q_4
-1	0.55	5000	-1267	-390	-1686
		(5077)	(-723)	(-1143)	(-1346)
	0.40	2433	-383	-363	-941
		(1857)	(-36)	(-568)	(-650)
	0.25	713	28	-206	-357
		(532)	(86)	(-214)	(-276)
	0.10	82	26	-37	-60
		(66)	(24)	(-32)	(-51)
-2	0.55	8131	-1401	-1091	-3149
	0.40	4481	-555	-784	-1803
	0.25	1401	67	-413	-709
	0.10	164	52	-74	-120
$+1$	0.55	-5289	1436	202	2013
	0.40	-2846	564	292	1134
	0.25	-742	-16	203	368
	0.10	-82	-26	37	60
$+2$	0.55	-8527	1628	692	3887
	0.40	-5798	1064	576	2518
	0.25	-1514	-21	402	752
	0.10	-164	-52	74	120

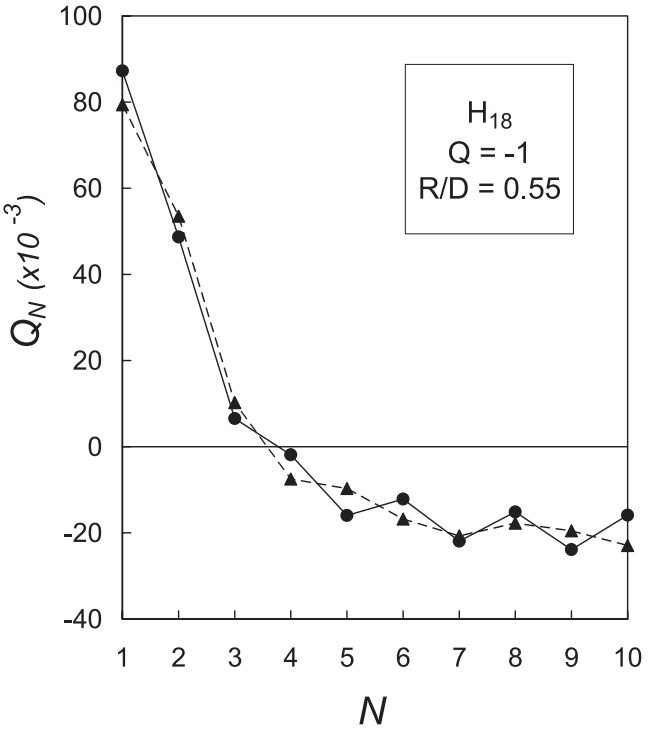

Fig. 1. Comparison of atomic charges (10^{-3} e$^-$) between classical macroscopic and microscopic quantum (in the Natural Orbital definition) calculations for a 18 hydrogen atoms ring cluster interacting with a $Q = -1$ point charge at a relative distance $R/D = 0.55$. Solid line: microscopic approach; dashed line: macroscopic approach.

$R/D = 0.7$ (not represented), invisible for $R/D = 0.55$ (Fig. 5). One may assume, but this hypothesis remains to be verified, that the microscopic oscillations could be smoothed when considering the higher electric multipoles: dipole $\mathbf{P}$, quadrupole $\mathbf{U}$, etc. In fact, we know [11] that the spatial average of the charge defined after a microscopic distribution of multipoles is given by $\rho - \nabla \cdot \mathbf{P} + \nabla^2 : \mathbf{U} - \ldots$

Slight oscillations also appear on several macroscopic curves. They are an artefact of the method of calculation, since they appear only when the residue $\Delta/\Delta_{\text{initial}}$ (see Eqs. (4) and (10)) is not zero. The oscillations are present when Q is close ($R/D = 0.55$, $\Delta/\Delta_{\text{initial}}$ between 2 and 3%; Figs. 1, 3, 5, 6), and disappear for $R/D = 0.4$ or less ($\Delta/\Delta_{\text{initial}} < 1\%$; Figs. 2, 4). Being meaningless, these oscillations must not be taken into account in the comparison.

(ii) Let us compare NPA with other definitions of the atomic charges. For $N = 18$, $Q = -1$ and $R/D = 0.4$, atom 1 bears 0.0296 e$^-$ after the Natural Orbital analysis, 0.0462 e$^-$ after the Mulliken analysis, 0.0374 e$^-$ derived from the electrostatic potential following Breneman et al. [12], 0.0245 e$^-$ in the derivation from the electrostatic potential by Kollman et al. [13], and 0.0300 e$^-$ from the *Atoms In Molecules* method (AIM) [14]. AIM is a powerful, although occasionally time-consuming, method of obtaining relevant partitions of the electronic cloud. Along the ring, the AIM method gives atomic charges in

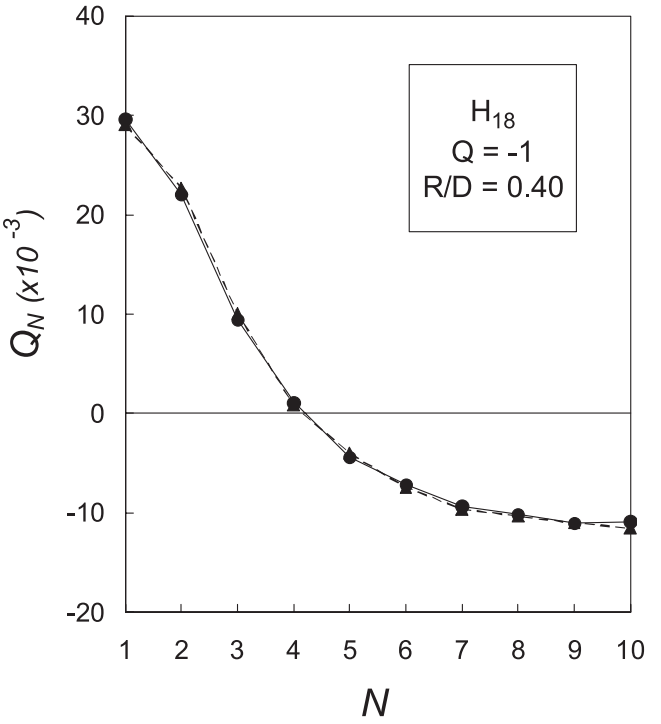

Fig. 2. A 18 hydrogen atoms ring cluster interacting with a $Q = -1$ point charge at a relative distance $R/D = 0.40$ (same symbols as in Fig. 1).

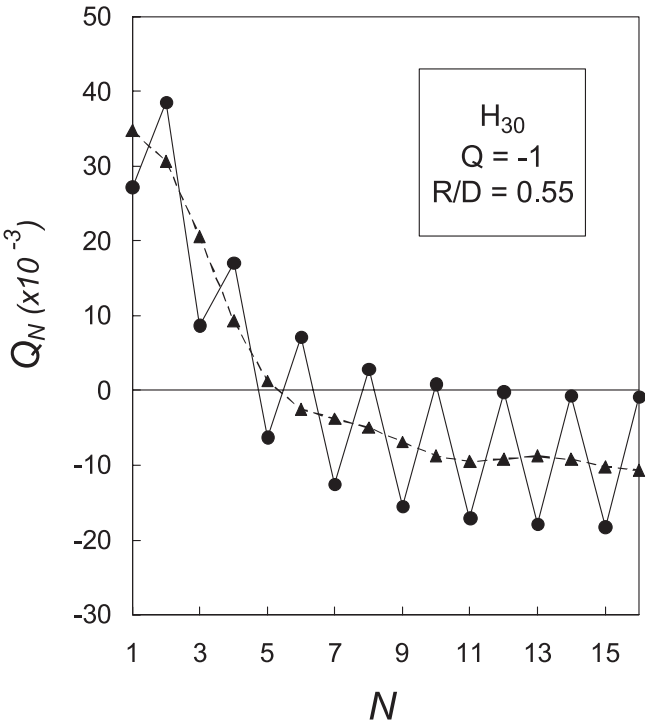

Fig. 3. A 30 hydrogen atoms ring cluster interacting with a $Q = -1$ point charge at a relative distance $R/D = 0.55$ (same symbols as in Fig. 1).

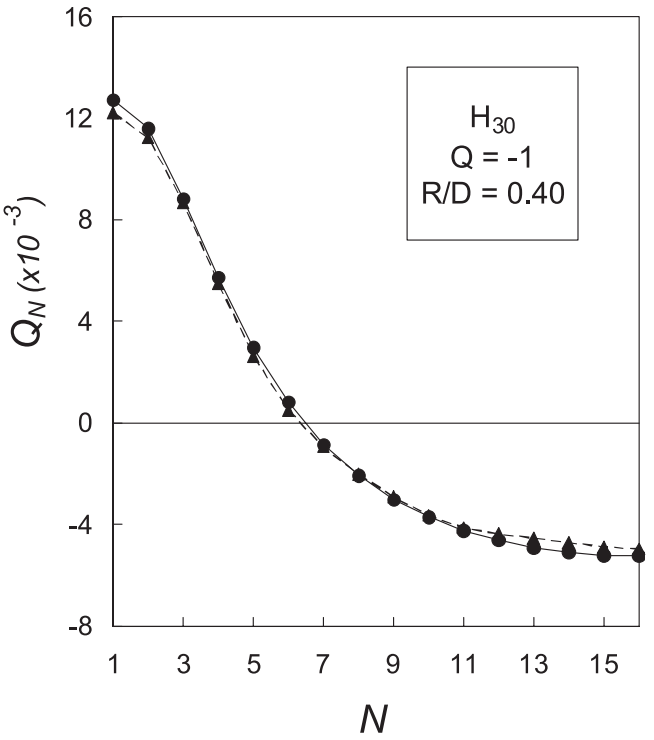

Fig. 4. A 30 hydrogen atoms ring cluster interacting with a $Q = -1$ point charge at a relative distance $R/D = 0.40$ (same symbols as in Fig. 1).

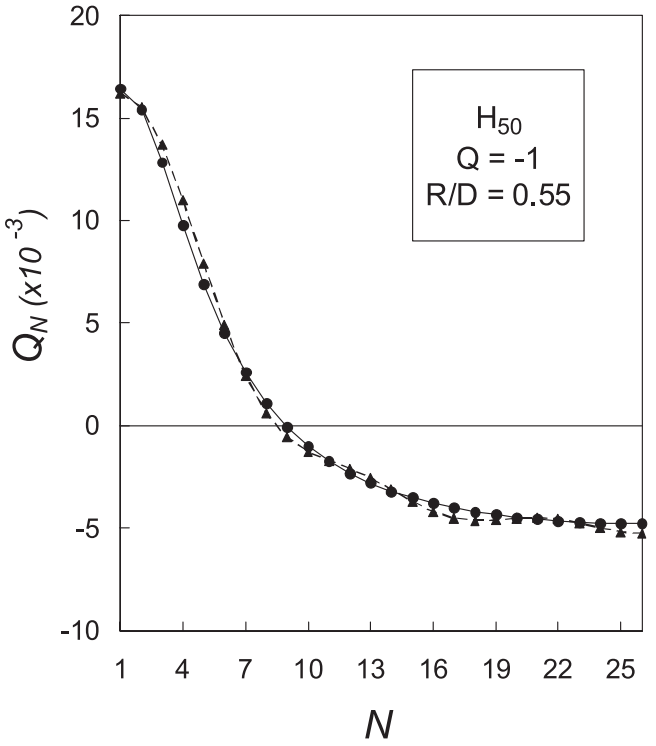

Fig. 5. A 50 hydrogen atoms ring cluster interacting with a $Q = -1$ point charge at a relative distance $R/D = 0.55$ (same symbols as in Fig. 1).

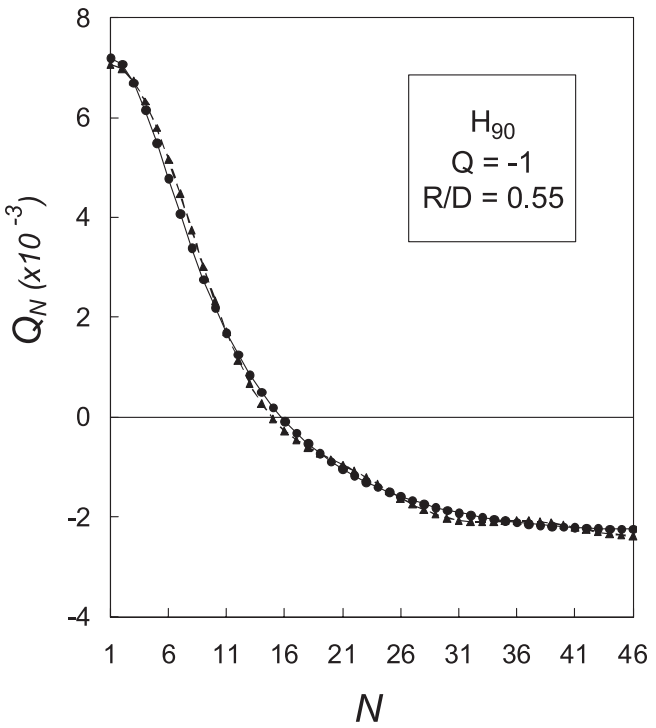

Fig. 6. A 90 hydrogen atoms ring cluster interacting with a $Q = -1$ point charge at a relative distance $R/D = 0.55$ (same symbols as in Fig. 1).

Table 3. Comparison between atomic charges (10^{-4} e$^-$) obtained from Natural Orbitals quantum microscopic and macroscopic calculations in the case of a [$N = 18$; $R/D = 0.40$] torus cluster of hydrogen and sodium atoms. The torus is influenced by a fixed $Q = -1$ (e$^-$) point charge lying at a distance D from the centre. diff and γ are defined by equations (15) and (16).

		Q_1	Q_2	Q_9	Q_{10}
H	mic	296	221	−110	−109
	mac ($\gamma = 1.0$)	291	227	−110	−115
	diff (%)	1.7	2.7	0	5.5
Na	mic	369	268	−130	−124
	mac ($\gamma = 1.0$)	291	227	−110	−115
	diff (%)	21	15	15	7.2
	mac ($\gamma = 1.35$)	362	277	−129	−136
	diff (%)	1.9	3.3	0.8	9.7

close agreement to the NPA method, both in sign and magnitude. The Mulliken analysis also gives values close to NPA, except on the first atom where the discrepancy is concentrated. The charge on atom 4 seems better when derived from the NPA definition (0.0011 e$^-$) than from the Mulliken definition (−0.0017 e$^-$). Indeed this atom lies still in the interaction cone of the negative point charge Q and should be positively charged a priori. Nevertheless these values are small. The derivation of Breneman et al. gives oscillations of charges between Q_7 to Q_{10}, while no oscillations are detected at this distance with NPA. The MKS derivation breaks the symmetry and charges are not satisfactory at all.

4.2 Sodium atom conductor

Since the main part of the physics which drives these properties seems to be already present in small size clusters, we only give the results corresponding to a $N = 18$ sodium atoms torus (and a $Q = -1$ point charge). First the structure of the isolated torus has been optimized in quantum calculations, leading to the values: $R = 9.8948$ Å, $R/N = 0.5497$, d(Na–Na) = 3.4364 Å and the atomization energy per atom $E_{\rm at}/N = 6.09$ kcal/atom. As for hydrogen rings the distance d is larger than both the diatom and the solid state distance.

The results are similar for sodium and for hydrogen atoms, but the agreement between the microscopic and macroscopic charges is not as good for Na as it was for H. This is apparent for $R/D = 0.4$ (Tab. 3): for atoms 1 and 2, and 9 and 10 at the opposite on the ring, the relative difference

$$\text{diff} = |Q^{\rm mic} - Q^{\rm mac}|/Q^{\rm mic} \tag{15}$$

is higher for Na than for H. The macroscopic calculations give the same charges for Na and H, since the radii R and r of the torus are in the same proportion for Na as for H. Indeed, in both cases we have chosen r equal to half the interatomic distance. This choice $r = d/2$ of the torus

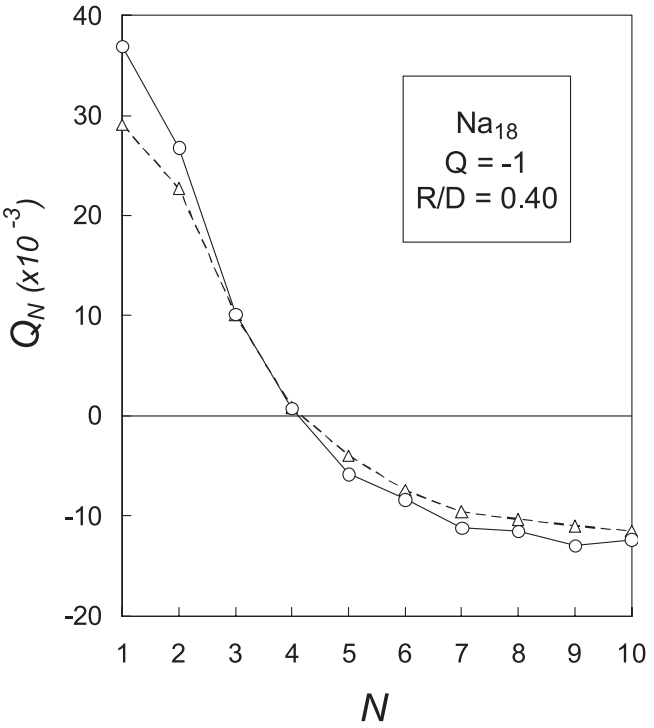

Fig. 7. A 18 sodium atoms ring cluster interacting with a $Q = -1$ point charge at a relative distance $R/D = 0.40$ (same symbols as in Fig. 1).

section radius happened to be satisfactory for hydrogen, but clearly it is not for sodium. When we try other section radii r defined by

$$r = \gamma d/2, \tag{16}$$

with a proportionality factor γ different from 1 (Fig. 8), we obtain the best agreement for $\gamma = 1.35$ (Tab. 3), i.e. $r = 2.32$ Å. This study was repeated for $R/D = 0.55$, leading to similar conclusions. The difference between γ(H) = 1.0 and γ(Na) = 1.35 can be explained partly by the shortness of the distance d(Na-Na) in the ring. Indeed, let us compare r not to $d/2$ like in (16), but to the covariant radius $\mathrm{d_{diatom}}/2$ measured in the diatomic molecule as usual:

$$r = \gamma' d_{\rm diatom}/2.$$

Then the proportionality factors γ' are $\gamma'(H) = 0.484/0.373 = 1.30$ and $\gamma'(\mathrm{Na}) = 2.32/1.858 = 1.25$.

5 Conclusion

In the present study of the electrostatic influence, we have chosen a simple microscopic conductor model, which certainly does not exactly describe a real conductor. But this simplicity has allowed us to apply ab initio calculations without any of the strong approximations that are commonly used for conducting materials.

For all cluster sizes in the microscopic calculations we observed oscillations in charge magnitudes from one given

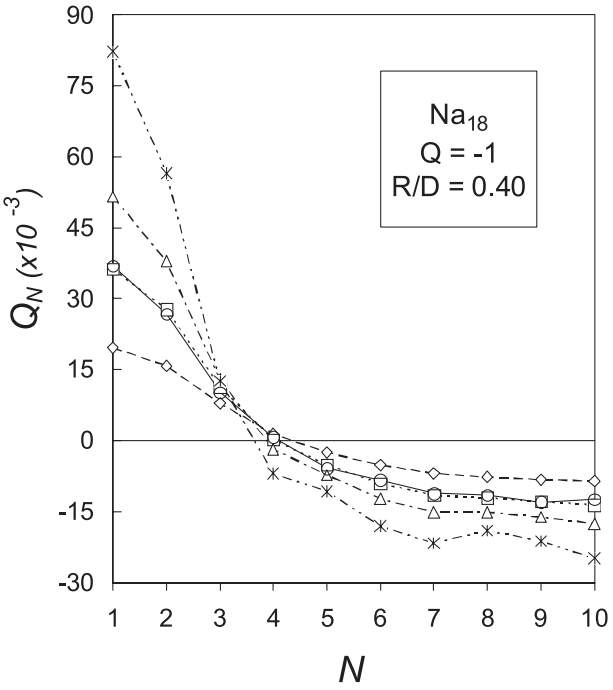

Fig. 8. A 18 sodium atoms ring cluster interacting with a $Q = -1$ point charge at a relative distance $R/D = 0.40$, for various values of the proportionality factor γ defined by equation (16). ◇: $\gamma = 0.5$; □ : $\gamma = 1.35$; $\Delta = 2.0$; X: $\gamma = 3.0$; O: microscopic results.

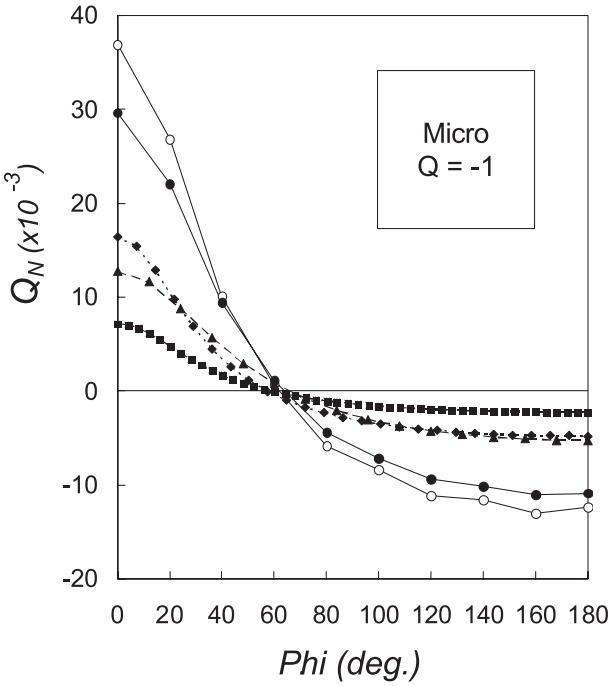

Fig. 9. Comparison between atomic electronic charges obtained from microscopic quantum calculations (in the Natural Orbital definition) for different sizes of clusters in interaction with a $Q = -1$ point charge lying at different R/D distances, in function of the angle at the centre. O: Na_{18}; $R/D = 0.40$; •: H_{18}; $R/D = 0.40$; ▲: H_{30}; $R/D = 0.40$; ♦: H_{50}; $R/D = 0.55$; ■ : H_{90}; $R/D = 0.55$.

atom to its neighbours. Their amplitude is greater when the external charge is close (i.e. R/D tends to one), which can be explained by the strong perturbation in the electronic cloud.

The results obtained from different cluster sizes and R/D ratios are plotted and compared in Figures 9 and 10 in the microscopic and macroscopic cases respectively. They are given in function of φ, the angle at the centre of the torus joining the external point charge and a given atom. We do not consider the same R/D ratio for all cluster sizes but the ratio for which the microscopic oscillations disappear. Comparing the curves between Figures 9 and 10, where the same ordinate range has been used, the overall agreement is evident. All curves seem to cross the $Q_N = 0$ line at the same point around $\varphi = 60°$. The angles φ_T, corresponding to the tangent to the torus issued from the external point charge are 66° and 57° for R/D ratios equal to 0.40 and 0.55 respectively. The tangent point separates atoms positively charged from the negatively charged.

When considering Na instead of H atoms in macroscopic calculations, we needed to vary the radius of the torus section. The value of the proportionality factor γ, considered in relation (16), appears reasonable.

The agreement between the two approaches indicates that the Maxwell equations can be applied to such nanoscale systems [15]. As discussed on the $N = 6$ cluster, the linearity constraint is a problem only when the external charge lies close to the torus.

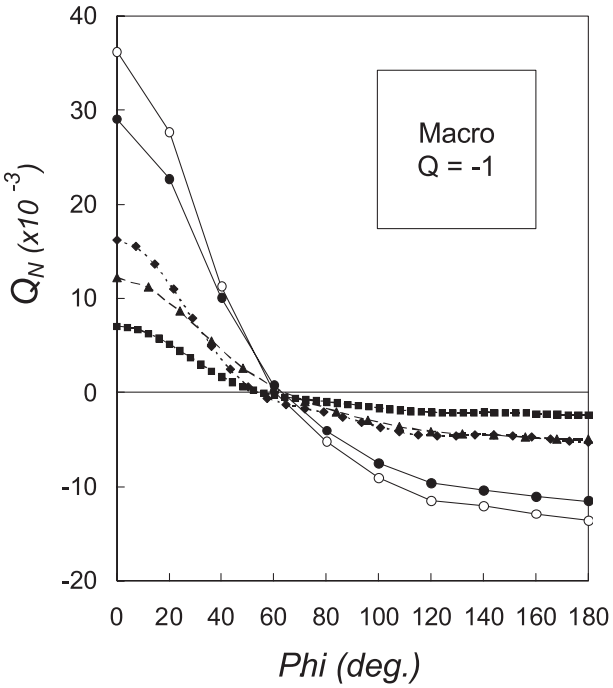

Fig. 10. Comparison between atomic charges obtained from classical macroscopic equations for different sizes of clusters in interaction with a $Q = -1$ point charge lying at different R/D distances, in function of the angle at the centre (same symbols as in Fig. 9).

We thank Prof. Stephane Humbel, Univ. Paul-Cezanne, Marseilles, for computing time provided on his cluster of processors. We are indebted to a referee for helpful criticisms.

References

1. J.D. Jackson, *Classical electrodynamics*, 2nd edn. (Wiley, New York, 1975)
2. M. Hagiescu-Miriste, A. Hagiescu-Miriste, Romanian Rep. Phys. **57**, 177 (2005)
3. G. Iannaccone, M. Macucci, E. Amirante, Y. Jin, H. Lanois, C. Vieu, Superlattice Microstruct. **27**, 369 (2000)
4. S.V. Rotkin, V. Shrivastava, K.A. Bulashevich, N.R. Aluru, Int. J. Nanosc. **1**, 337 (2002)
5. I.S. Gradshteyn, I.M. Ryzhik, *Table of integrals, series, and products* (Academic Press, London, 1980)
6. M. Abramowitz, I.A. Stegun, *Handbook of mathematical functions with formulas, graphs, and mathematical tables* (National Bureau of Standards, Washington, 1972)
7. J.B. Foresman, Æ. Frisch, *Exploring chemistry with electronic structure methods*, 2nd edn. (Gaussian Inc., Pittsburgh, PA, USA, 1996), p. 194
8. R. Ditchfield, W.J. Hehre, J.A. Pople, J. Chem. Phys. **54,** 724 (1971); W.J. Hehre, R. Ditchfield, J.A. Pople, J. Chem. Phys. **56**, 2257 (1972); P.C. Hariharan, J.A. Pople, Mol. Phys. **27**, 209 (1974); M.S. Gordon, Chem. Phys. Lett. **76**, 163 (1980); P.C. Hariharan, J.A. Pople, Theor. Chim. Acta **28**, 213 (1973); R.C. Binning Jr., L.A. Curtiss, J. Comp. Chem. **11**, 1206 (1990)
9. E.D. Glendening, A.E. Reed, J.E. Carpenter, F. Weinhold, NBO (Version 3.1); J.E. Carpenter, F. Weinhold, J. Mol. Struct. Theochem **169**, 41 (1988); J.E. Carpenter, PhD thesis (University of Wisconsin, Madison, WI, USA, 1987); J.P. Foster, F. Weinhold, J. Am. Chem. Soc. **102**, 7211 (1980); A.E. Reed, F. Weinhold, J. Chem. Phys. **78**, 4066 (1983); A.E. Reed, R.B. Weinstock, F. Weinhold, J. Chem. Phys. **83**, 735 (1985); A.E. Reed, L.A. Curtiss, F. Weinhold, Chem. Rev. **88**, 899 (1988)
10. M.J. Frisch, G.W. Trucks, H.B. Schlegel, G.E. Scuseria, M.A. Robb, J.R. Cheeseman, V.G. Zakrzewski, J.A. Montgomery, R.E. Stratmann, J.C. Burant, S. Dapprich, J.M. Millam, A.D. Daniels, K.N. Kudin, M.C. Strain, O. Farkas, J. Tomasi, V. Barone, M. Cossi, R. Cammi, B. Mennucci, C. Pomelli, C. Adamo, S. Clifford, J. Ochterski, G.A. Petersson, P.Y. Ayala, Q. Cui, K. Morokuma, D.K. Malick, A.D. Rabuck, K. Raghavachari, J.B. Foresman, J. Cioslowski, J.V. Ortiz, B.B. Stefanov, G. Liu, A. Liashenko, P. Piskorz, I. Komaromi, R. Gomperts, R.L. Martin, D.J. Fox, T. Keith, M.A. Al-Laham, C.Y. Peng, A. Nanayakkara, C. Gonzalez, M. Challacombe, P.M.W. Gill, B.G. Johnson, W. Chen, M.W. Wong, J.L. Andres, M. Head-Gordon, E.S. Replogle, J.A. Pople, *GAUSSIAN 98*, Revision A9 (Gaussian Inc., Pittsburgh PA, USA, 1998)
11. B. Blaive, J. Metzger, J. Phys. France **42**, 1533 (1981)
12. L.E. Chirlian, M.M. Francl, J. Comp. Chem. **8**, 894 (1987); C.M. Breneman, K.B. Wiberg, J. Comp. Chem. **11**, 361 (1990)
13. B.H. Besler, K.M. Merz Jr., P.A. Kollman, J. Comp. Chem. **11**, 431 (1990); U.C. Singh, P.A. Kollman, J. Comp. Chem. **5**, 129 (1984)
14. R.F.W. Bader, *Atoms in Molecules: A Quantum Theory* (Oxford Univ. Press, Oxford, UK, 1990)
15. V. Martynov, B. Vidal, P. Vincent, M. Brunel, D.V. Roschupkin, Yu. Agafonov, A. Erko, A. Yuakshin, Nucl. Instrum. Meth. A **339**, 617 (1994).